



Selective transepithelial ablation with simultaneous accelerated corneal crosslinking for corneal regularization of keratoconus: STARE-X protocol

Miguel Rechichi, MD, PhD, Cosimo Mazzotta, MD, PhD, Giovanni William Oliverio, MD, Vito Romano, MD, Davide Borroni, MD, Marco Ferrise, MD, Simone Bagaglia, MD, Soosan Jacob, MS, FRCS, DNB, Alessandro Meduri, MD, PhD

Purpose: To evaluate the changes in refractive outcomes and corneal aberrations in central and paracentral keratoconus after selective transepithelial topography-guided photorefractive keratectomy combined with accelerated corneal crosslinking (STARE-X).

Settings: Centro Polispecialistico Mediterraneo, Siena Crosslinking Center, and University of Messina, Italy.

Design: Prospective, interventional, multicentric study.

Methods: Patients were subdivided into 2 groups: Group 1 with cone located within the central 3 mm zone (50 eyes) and Group 2 (50 eyes) with cone located outside the central 3 mm zone. Follow-up was 2 years at least for all eyes. Outcome parameters included uncorrected distance visual acuity (UDVA) and corrected distance visual acuity (CDVA). Corneal tomography and corneal wavefront aberrations were assessed and compared before and 2 years after the treatment.

Results: 100 eyes of 100 patients underwent STARE-X protocol. At 2 years, UDVA and CDVA improved, and sphere, cylinder, and Kmax reduced after treatment in both groups ($P < .001$, respectively). Moreover, a statistically significant reduction was observed of total higher-order aberrations root mean square (RMS), coma RMS, and spherical aberration RMS in both groups ($P < .001$, respectively). However, CDVA improved more in Group 1 than in Group 2 ($P < .02$).

Conclusions: The STARE-X protocol demonstrated effective results in halting keratoconus progression and improving corneal regularity with a safe and effective profile. STARE-X improved both visual acuity and corneal aberration at 2 years. Longer follow-up studies are warranted to observe further long-term CXL flattening effect on the cone.

J Cataract Refract Surg 2021; 47:1403–1410 Copyright © 2021 The Author(s). Published by Wolters Kluwer Health, Inc. on behalf of ASCRS and ESCRS

The effectiveness of corneal crosslinking (CXL) to stop the keratoconus (KC) progression has been confirmed in long-term studies, demonstrating also an improvement in visual acuity, topographic, and aberrometric outcomes; however, these results were commonly unpredictable and variable.^{1–3} The actual challenge in the management of keratoconus is to improve the refraction in patients with significant ectasia and high level of higher-order aberrations (HOAs).⁴ The way to improve visual acuity and quality of vision could be the corneal reshaping, regularizing as

much as possible the corneal geometry in the central 4 mm zone, and aiming to reduce vertical asymmetry and HOAs.⁵

Although the treatment of corneas with keratoconus using excimer laser machine was historically considered not appropriate for the risk of iatrogenic ectasia worsening, recent improvements in laser technology such as the development of topography-guided and wavefront-guided photorefractive keratectomy (PRK) procedures, supported by a state-of-art eye-tracking system that compensates XYZ and cyclorotation eye movement, have led to several

Submitted: October 12, 2020 | Final revision submitted: March 1, 2021 | Accepted: March 3, 2021

From the Centro Polispecialistico Mediterraneo, Sella Marina, Italy (Rechichi, Ferrise); Siena Crosslinking Center, Siena University Hospital, Ophthalmology Unit, Siena, Italy (Mazzotta, Bagaglia); Department of Biomedical Sciences, Ophthalmology Clinic, University of Messina, Messina, Italy (Oliverio, Meduri); Department of Ophthalmology, Royal Liverpool University Hospital, Liverpool, United Kingdom (Romano); Department of Ophthalmology, Riga Stradins University, Riga, Latvia (Borroni); Dr. Agarwal's Eye Hospital and Eye Research Centre, Chennai, India (Jacob).

Presented in part at the XXI AICCCER Congress, Bari, Italy, March 2018 and at AAO 2014, Chicago, Illinois, October.

Corresponding author: Oliverio Giovanni William, MD, Biomedical Department, Ophthalmology Clinic, University of Messina, Via Consollare Valeria 1, Messina, Italy 98124. Email: giovannioliverio89@gmail.com.

options for dealing with irregular and keratoconic corneas, introducing the concept of customized treatments.^{6–8}

The target of customized ablation is to improve the quality of visual acuity reducing not only the lower-order aberrations but also the higher-order aberration and irregular corneal astigmatism. Several approaches were proposed, combining different protocols of CXL and refractive treatment (CXL plus) performed at the same time or in 2 steps, reporting a significant reshaping of the irregular corneal surface and improvement of the visual function.^{9–14}

In this study, we describe a new procedure of selective transepithelial ablation for the regularization of keratoconic cornea and simultaneous accelerated corneal crosslinking (STARE-X). The aim of this study was to evaluate the changes in refractive and corneal aberration outcomes at 2 years, in eyes with progressive keratoconus, treated with STARE-X protocol.

Furthermore, several authors showed that cone location is one of the most important parameters involved in corneal flattening after CXL performed with the standard protocol.^{15,16} Therefore, to evaluate the cone location effect on the outcomes, we compared the results of the STARE-X protocol in central and paracentral keratoconus locations.

METHODS

This prospective interventional multicentric study involved 100 eyes of 100 patients with progressive grades I and II keratoconus (Amsler-Krumeich classification). All patients provided informed consent, after receiving an explanation of the nature and objective of the study. This study was approved by the local ethical committee of the University of Messina and was conducted according to the tenets of the Declaration of Helsinki. The treatments and data collection were performed at the Siena Crosslinking Centre (Siena, Italy), at Centro Polispecialistico Mediterraneo (Sella Marina, Italy), and at the Refractive Unit of the University of Messina (Messina, Italy).

The inclusion criteria were as follows: aged 21 years or older, grades I and II keratoconus (Amsler-Krumeich classification), progressive keratoconus (defined as an increase of at least 1.00 diopter [D] in Kmax over the 12 months preceding the treatment), the requirement of visual quality improvement, rigid gas-permeable contact lens intolerance or altered fitting, corrected distance visual acuity (CDVA) of 20/40 or less or 0.6 decimal Snellen lines or less, Kmax of 55.00 D or less, optical thinnest point pachymetry of 400 μm or greater. The exclusion criteria were as follows: ocular infections, a history of interstitial keratitis, herpes simplex keratitis, or other autoimmune diseases, presence of corneal scars, and any previous corneal procedure.

All patients underwent preoperatively a full ophthalmologic evaluation, including measurement of uncorrected distance visual acuity (UDVA), CDVA, sphere, cylinder, slitlamp evaluation, and tonometry. Topographic, pachymetric, and aberrometric data were assessed using the Sirius topography system (Costruzione Strumenti Oftalmici). Minimum corneal thickness (MCT), Kmax, flattest keratometric reading (K1), steepest keratometric reading (K2), Q value, total HOAs root mean square (HOAs RMS), coma RMS, and spherical aberration (SA) RMS were assessed with an analysis zone of 6 mm diameter. Anterior segment OCT (RTVue, OptoVue, Inc.) was used to evaluate the corneal thinnest point and demarcation line depth after treatment. The same measurements were performed at the baseline and at 3 months, 6 months, 12 months, and 24 months.

The steepest tangential curvature on corneal topography was used for classifying the cones. The distance from the geometric center was used to divide the eyes into 2 groups preoperatively: Group 1, cones located within the central 3 mm zone, and Group 2, cones located outside the central 3 mm zone. Fifty eyes (Group 1) had Kc more than 50% within 3 mm on the anterior tangential map, and 50 eyes (Group 2) had Kc less than 50% within 3 mm on the anterior tangential map.

Statistical Analysis

The numerical data are expressed as mean and SD and the categorical variables as absolute frequency and percentage. The fitting of the data to a normal distribution was tested by the Kolmogorov-Smirnov test. The preoperative and postoperative values of the variables of Groups 1 and 2 were compared using the χ^2 test for categorical variables, the *t* test for parametric data, and the Mann-Whitney *U* test for nonparametric data. The postoperative outcomes were compared with preoperative values within each group using the Wilcoxon signed-rank test and *t* test for paired data.

The sample size was estimated using mean preoperative keratometry (K1 and K2) and considering an α error of 0.05 and a β error of 80%, and the required sample size to detect differences between the 2 groups was 84 patients. Therefore, 100 patients were enrolled to allow a possible drop out.

To analyze the outcomes in subgroups according to the baseline CDVA, it was considered the median value of 0.33 logMAR; for each group, patients with CDVA more than 0.33 logMAR were included in the low-vision subgroup, whereas patients with CDVA of 0.33 logMAR or less were included in the high-vision subgroup. Multiple regression analysis was performed to evaluate the influencing factors of the final CDVA, considering the baseline UDVA, CDVA, refractive errors, Kmax, and MCT as independent variables and CDVA at 2 years as dependent variable. A *P* value less than 0.05 was considered statistically significant. All statistical analyses and sample size calculations were performed with IBM SPSS Statistics for Windows software (v. 24.0; IBM Corp.).

Laser Platform

The excimer laser platform was a Schwind Amaris 500 platform (Schwind eye-tech-solutions GmbH & Co. KG) linked with anterior segment Scheimpflug tomography with integrated Placido topography–Scheimpflug and pupillometry (Sirius, Costruzione Strumenti Oftalmici). The laser works at a true repetition rate of 500 Hz and produces a beam size of 0.54 mm full-width at half-maximum with a super Gaussian spot profile. High-speed eye tracking (pupil and limbus tracker with cyclotorsional tracking) with a 1050 Hz acquisition rate is completed within a latency time of 3 ms.⁷ The crosslinking device used was the KXL UV-A source (Avedro, Inc.).

Selective Transepithelial Ablation for Regularization of Ectasia and Simultaneous Crosslinking

First Step: Excimer Laser Corneal Regularization The procedure consists of single-step corneal topography-guided transepithelial PRK with a starting planned optical zone of 7 plus 0.6 mm transition zone for central cone and 6.5 mm optical zone plus 0.5 mm transition zone for peripheral cone. All treatments were planned by topographic data derived from the Optimized Refractive Keratectomy-Custom Ablation Manager software (ORK-CAM 5.1, Schwind eye-tech-solutions GmbH & Co. KG), considering the manifest refraction of the patient, corneal pachymetry, and aberrometric and topographic parameters.

The eye tracker was checked intraoperatively before starting the treatment, considering the iris images taken in a supine position, to compensate for the cyclorotation that happens when a patient assumes a supine position, and comparing these preoperative images with repetitive images acquired throughout the treatment to determine the dynamic cyclotorsion.

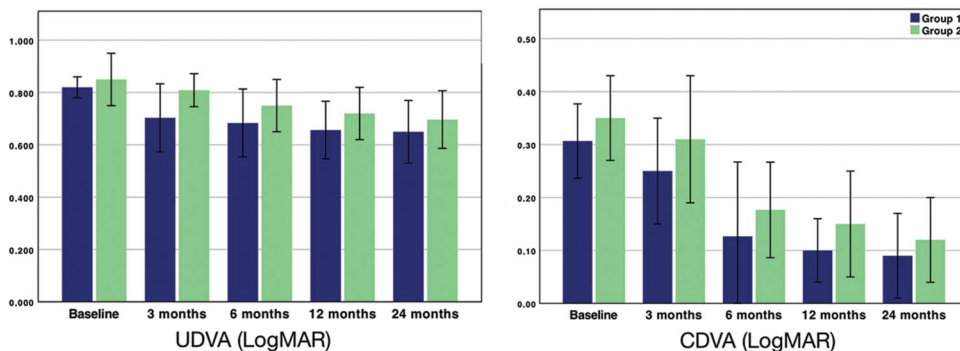


Figure 1. UDVA and CDVA preoperatively and at 24 months after treatment.

To realize an ablation precisely aligned with the preoperative plan, the dynamic cyclotorsion control compensated the cyclorotation with the rotation of the ablation profile. The principal parameters of the STARE-X protocol for the corneal regularization of keratoconus are the following sequent: epithelium removal of 55 μm in the center and 65 μm in the periphery of the selected ablation zone; stromal ablation depth limited at 50 μm , and optimized by excimer laser software for saving tissue; maximum correction of coma aberration, eventually limiting spherical and cylinder correction to not exceed the stromal ablation depth limit; and ablation offset up to 1 mm from corneal vertex in the direction of the cone apex as measured manually on topography.

Second Step: Customized Energy-Pulsed Accelerated CXL. After excimer treatment, eyes underwent an epithelium-off pulsed-light accelerated corneal crosslinking by using the KXL UV-A source (Avedro, Inc.). The target residual stromal thickness (RST), planned before laser excimer ablation, was considered to choose the UV-A irradiation power and dose for CXL treatment.

The pulsed UV-A irradiation for 16 minutes, with 15 mW/cm^2 , pulsed 2:1 second, and 5.4 J dose energy was considered if the RST was more than 400 μm and pulsed UV-A irradiation for 8 minutes, with 30 mW/cm^2 and 7.2 J dose energy if the RST was less than 400 μm . The beam was carefully centered on the cone apex evaluated at the anterior tangential map for all the treatments.

A dextran-free riboflavin 0.1% with hydroxylpropyl methyl cellulose (VibeX Rapid; Avedro, Inc.) was used, with 10 minutes of corneal soaking. Treated eyes were dressed by a soft contact lens

bandage for 3 days and medicated with netilmicin 0.3% eyedrops (Nettacin, Sifi Medtech Srl) 3 times daily, bromfenac 0.9 mg/mL eyedrops (Yellox, Bausch & Lomb, Inc.) 2 times daily, trehalose 30 mg/mL and sodium hyaluronate 1.5 mg/mL eyedrops (Thealoz Duo, Théa Pharma GmbH) 4 times daily, and loteprednol etabonate 0.5% (Lotemax, Bausch & Lomb, Inc.) 3 times daily for 7 days.

RESULTS

A total of 100 patients with keratoconus were included in this study: 50 eyes of 50 patients (35 men, 15 women) presented a central cone location (Group 1), and 50 eyes of 50 patients (31 men, 19 women) presented a paracentral cone location (Group 2). The baseline clinical and demographics characteristics of the study population are reported in Table 1. The mean age of the patients was 32 ± 6.1 years in Group 1 and 30.9 ± 7.5 years in Group 2. All patients enrolled in the treatment completed the 24-month follow-up.

The mean intended central ablation depth in this series was 47.5 ± 11.4 μm , and the mean changes in central and minimal pachymetry were 53.7 ± 20.5 μm and 56.7 ± 24.3 μm , respectively. The mean stromal ablation depth was 45.4 ± 12.6 μm ; the mean optical zone and the total ablation zone planned was 6.8 ± 0.3 mm and 7.4 ± 0.2 mm in central group and 6.2 ± 0.2 mm and 6.9 ± 0.3 mm in paracentral group, respectively.

Refractive and Aberrometric Outcomes

After treatment, a significant improvement was observed in UDVA and CDVA in both groups ($P < .001$ respectively),

Variable	Group 1 (N = 50)	Group 2 (N = 50)	P value
Age (y)	32 ± 6.15	30.9 ± 7.53	.38
M/F ratio	35:15	31:19	.56
UDVA (logMAR)	0.82 ± 0.15	0.85 ± 0.37	.65
CDVA (logMAR)	0.31 ± 0.07	0.35 ± 0.08	.48
Sphere (D)	-4.56 ± 1.98	-1.2 ± 2.25	<.0001*
Astigmatism (D)	-5.12 ± 2.69	-4.80 ± 1.40	.002*
K1 (D)	48.9 ± 1.07	45.95 ± 1.08	.98
K2 (D)	53.17 ± 1.07	49.8 ± 1.08	.47
Kmax (D)	54.5 ± 1.47	54.1 ± 0.65	.42
MCT (μm)	489.3 ± 32.6	467 ± 24.3	.001*
Coma RMS (μm)	1.68 ± 0.37	2.01 ± 0.52	.11
SA RMS (μm)	-1.12 ± 0.82	-0.18 ± 0.69	<.0001*
Total HOAs RMS (μm)	3.01 ± 0.41	3.85 ± 0.65	.0004*

Coma RMS = coma root main square; HOAs RMS = HOAs root main square; MCT = minimum corneal thickness; SA RMS = spherical aberration root main square

All data were reported as mean \pm SD

*Statistically significant

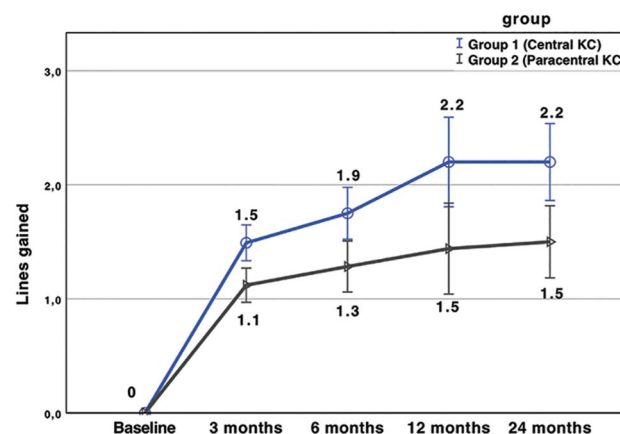


Figure 2. Results about Snellen lines gained in corrected distance visual acuity after treatment.

Variable	Group 1					P value ^a
	Preop	3 mo	6 mo	12 mo	24 mo	
UDVA	0.82 ± 0.15	0.69 ± 0.17	0.67 ± 0.18	0.65 ± 0.21	0.65 ± 0.31	<.001*
CDVA	0.31 ± 0.07	0.08 ± 0.06	0.08 ± 0.05	0.09 ± 0.06	0.09 ± 0.08	<.001*
Sphere (D)	-4.56 ± 1.98	-2.18 ± 1.4	-2.15 ± 1.6	-2.13 ± 1.5	-2.12 ± 2.1	<.001*
Astigmatism (D)	-5.12 ± 2.69	-3.70 ± 1.51	-3.80 ± 1.47	-3.90 ± 1.36	-3.90 ± 2.34	<.001*
K1 (D)	48.90 ± 1.07	46.40 ± 1.27	46.50 ± 1.32	46.30 ± 0.95	46.10 ± 0.94	<.001*
K2 (D)	53.17 ± 1.07	52.60 ± 2.15	52.70 ± 1.95	52.70 ± 1.85	52.80 ± 1.73	.04*
Kmax (D)	54.50 ± 1.47	53.10 ± 1.65	53.20 ± 1.71	53.20 ± 1.21	53.40 ± 1.01	<.001*
Q value	-0.95 ± 0.42	-0.43 ± 0.21	-0.44 ± 0.22	-0.43 ± 0.22	-0.43 ± 0.21	<.001*
MCT (µm)	489.3 ± 32.6	412 ± 14.5	412 ± 14.4	410 ± 14.3	410 ± 14.3	<.001*
RST (µm)	379.2 ± 49.5	371.1 ± 51.2	373.5 ± 48.9	373.1 ± 49.2	371.5 ± 50.5	.38
Coma RMS	1.68 ± 0.37	0.84 ± 0.33	0.86 ± 0.32	0.87 ± 0.32	0.87 ± 1.18	<.001*
SA RMS	-1.12 ± 0.82	-0.13 ± 0.06	-0.13 ± 0.05	-0.12 ± 0.04	-0.12 ± 0.08	<.001*
Total HOAs RMS	3.01 ± 0.41	2.75 ± 0.36	2.76 ± 0.34	2.77 ± 0.34	2.79 ± 0.32	<.001*

Coma RMS = coma root main square; HOA RMS = HOAs root main square; Kmax = maximum keratometry; MCT = minimum corneal thickness; SA RMS = spherical aberration root main square. All data were reported as mean ± SD

^aPreoperative vs 24 months

*Statistically significant

starting from 3 months and lasting until the end of follow-up (Figure 1). These results showed a significant improvement in lines gained, with 2.2 lines in Group 1 and 1.5 in Group 2 (Figure 2).

A significant reduction of sphere and astigmatism was demonstrated in both groups postoperatively ($P < .001$ respectively); however, these changes were more evident in Group 1. At 24 months, the total HOAs RMS, coma RMS, and SA RMS significantly decreased in both groups ($P < .001$).

Corneal Morphological Changes

At 2 years, a significant decrease was observed in K1, K2, and Kmax after treatment in both groups (Table 2; Figure 3

and 4). In addition, at the end of follow-up, there was a significant decrease in Q value and MCT in both groups.

The corneal demarcation line was observed in all cases 1 month postoperatively, which measured at a mean of 231 ± 22 µm depth from the epithelium in Group 1 and 227 ± 32 µm in Group 2.

Comparison Between Groups 1 and 2

Preoperative spherical error and astigmatism were higher in Group 1 ($P < .0001$ and $P = .002$, respectively). Preoperative MCT was thinner in Group 2 ($P = .001$). SA RMS was higher in Group 1 ($P < .0001$), whereas total HOA RMS was more pronounced in Group 2 ($P = .0004$) (Table 1).

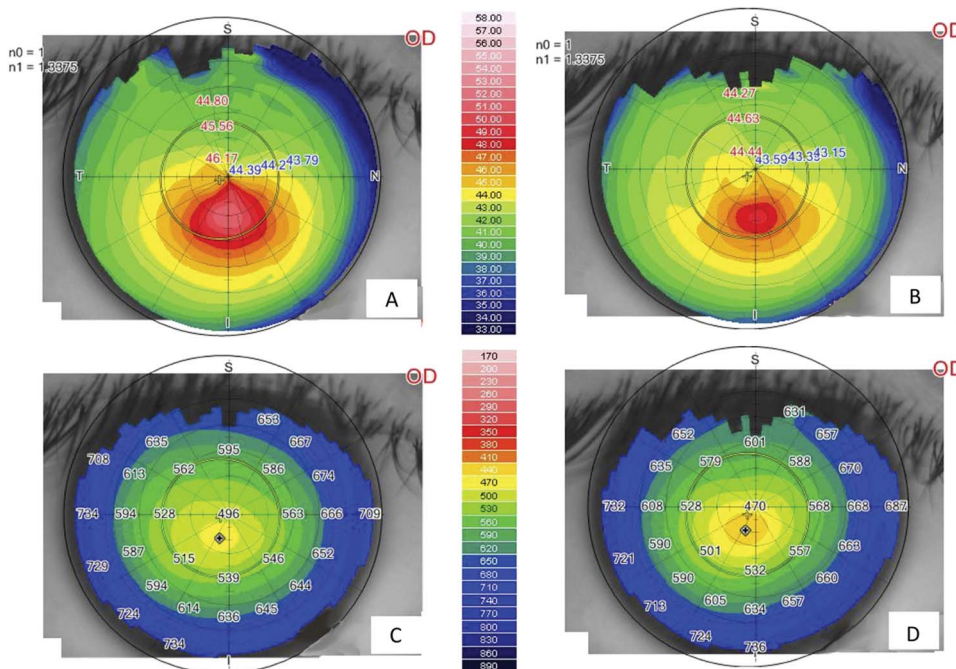


Figure 3. Anterior sagittal maps: baseline (A) and 1 year after STARE-X (B). Pachymetry maps: baseline (C) and 1 year after STARE-X (D).

Table 2. Continued					
Group 2					
Preop	3 mo	6 mo	12 mo	24 mo	P value ^a
0.85 ± 0.37	0.67 ± 0.22	0.69 ± 0.21	0.70 ± 0.24	0.70 ± 0.25	<.001*
0.35 ± 0.09	0.11 ± 0.06	0.11 ± 0.06	0.12 ± 0.04	0.12 ± 0.08	<.001*
-1.2 ± 2.25	-1.48 ± 1.14	-1.48 ± 1.14	-1.48 ± 1.14	-1.48 ± 1.74	<.001*
-4.80 ± 1.40	-4.60 ± 0.72	-4.60 ± 0.72	-4.60 ± 0.72	-4.60 ± 1.32	<.001*
45.95 ± 1.08	46.01 ± 1.08	46.01 ± 1.08	46.01 ± 1.08	46.01 ± 1.08	.22
49.80 ± 1.08	48.96 ± 0.81	48.96 ± 0.81	48.96 ± 0.81	48.96 ± 0.81	<.001*
54.10 ± 0.65	53.00 ± 0.91	53.00 ± 0.91	53.00 ± 0.91	53.00 ± 0.91	<.001*
-0.25 ± 0.18	-0.23 ± 0.19	-0.23 ± 0.18	-0.24 ± 0.18	-0.23 ± 0.18	.13
467 ± 24.3	467 ± 24.3	467 ± 24.3	467 ± 24.3	404.7 ± 15.1	<.001*
361.7 ± 47.5	362.3 ± 48.1	363.2 ± 47.9	362.7 ± 48.2	363.1 ± 48.2	.45
2.01 ± 0.52	2.01 ± 0.62	2.01 ± 0.62	2.01 ± 0.62	1.02 ± 0.39	<.001*
-0.18 ± 0.69	-0.18 ± 0.29	-0.18 ± 0.29	-0.18 ± 0.29	-0.16 ± 0.58	<.001*
3.85 ± 0.65	3.85 ± 0.45	3.85 ± 0.45	3.85 ± 0.45	2.83 ± 0.44	<.001*

At 2 years, a statistically significant difference of CDVA was noted between Groups 1 and 2 ($P = .02$); SA RMS was lower in Group 1 ($P = .04$) (Table 3).

Multiple regression analysis to evaluate the influences of baseline factors on the final CDVA at 2 years is reported in Table 4. The mean estimated RST during the treatment planning was $369.2 \pm 49.5 \mu\text{m}$ in Group 1 and $351.7 \pm 47.5 \mu\text{m}$ in Group 2; these did not change after 2 years (Table 2).

Subgroups Analysis

At 24 months, a statistically significant change in CDVA was observed in both low-vision and high-vision subgroups ($P < .001$) in Groups 1 and 2, respectively. A significant

reduction of Kmax and MCT was showed in both groups postoperatively ($P < .001$, respectively).

In addition, the aberrometric outcomes decreased in each group when evaluated at the end of the follow-up (Table 5). No statistically significant differences were observed when comparing central and paracentral keratoconus in patients with low-vision after treatment, whereas statistically significant differences were showed in astigmatism, Kmax, and MCT when comparing patients with high vision in Groups 1 and 2 (Table 5).

Safety and Complications

No intraoperative complications were observed during the treatment. Twenty-five patients (25%) reported

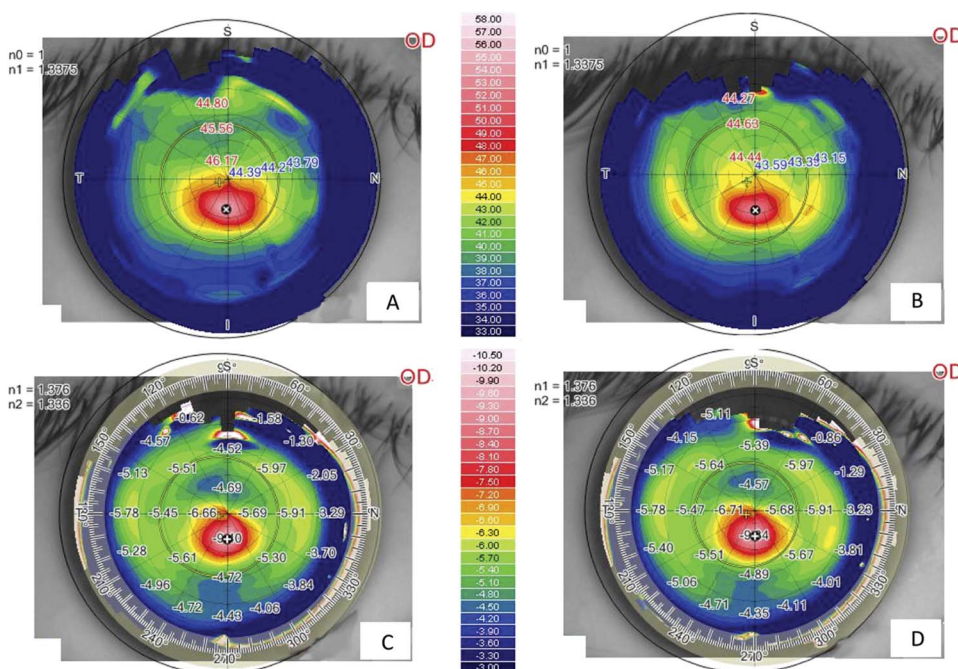


Figure 4. Anterior tangential maps: baseline (A) and 1 year after STARE-X (B). Posterior tangential maps: baseline (C) and 1 year after STARE-X (D).

Variable	Group 1	Group 2	P value
UDVA (logMAR)	0.65 ± 0.31	0.70 ± 0.25	.34
CDVA (logMAR)	0.09 ± 0.08	0.12 ± 0.09	.02*
Sphere (D)	-2.12 ± 2.10	-1.48 ± 1.74	.64
Astigmatism (D)	-3.90 ± 2.34	-4.60 ± 1.32	.64
K1 (D)	46.10 ± 0.94	46.01 ± 1.08	.76
K2 (D)	52.80 ± 1.73	48.96 ± 0.81	.21
Kmax (D)	53.40 ± 1.01	53.00 ± 0.91	.47
MCT (μm)	410 ± 14.3	404.7 ± 15.1	.67
Coma RMS (μm)	0.87 ± 1.18	1.02 ± 0.39	.77
SA RMS (μm)	-0.12 ± 0.08	-0.16 ± 0.58	.04*
Total HOAs RMS (μm)	2.79 ± 0.32	2.83 ± 0.44	.20

Coma RMS = coma root main square; HOA RMS = HOA root main square; Kmax = maximum keratometry; MCT = minimum corneal thickness; SA RMS = spherical aberration root main square

All data were reported as mean ± SD

*Statistically significant

significant pain during the first 2 days after treatment. In all patients, complete reepithelialization occurred 4 days after treatment. A mild corneal haze was observed in 13 patients (13%), which resolved without sequelae in all cases after the first 3 months. No

progression of keratoconus was documented up to 2 years of follow-up.

DISCUSSION

According to previous studies on CXL-plus treatment, we documented the effectiveness and safety of the new STARE-X protocol to improve visual acuity, manifest refraction, and aberrometric outcomes in patients with keratoconus at 2 years after treatment.¹⁰⁻¹³ Although the advantages of simultaneous or sequential PRK and CXL procedures are still controversial, the main benefit of combined procedures at the same time is to immediately regularize keratoconus and strengthen the remodeled cornea, which could further flatten in the following months.^{14,17}

The safety of the procedure is certainly correlated with the thickness of the residual stromal tissue as previous studies defined a maximum stromal ablation depth comprised between 50 μm and 80 μm, with an RST from 300 to 450 μm.¹⁷

On the other hand, the importance of the corneal epithelium is well documented to be acting as covering tissue smoothing the anterior elevation irregularities of the cornea.¹⁸⁻²⁰ In STARE-X procedure, to reduce the stromal thinning under the cone area, a customized epithelium

Variable	Paracentral			Central		
	β coefficient	95% CI	P value	β coefficient	95% CI	P value
Intercept	-0.22	-0.65, 0.19	.28	0.08	-0.48, 0.64	.77
UDVA	0.07	-0.07, 0.24	.31	-0.02	-0.11, 0.05	.50
CDVA	0.32	0.23, 0.42	<.0001*	0.06	0.02, 0.13	.04*
Sphere	-0.01	-0.02, -0.01	<.0001*	-0.01	-0.02, 0.002	.11
Astigmatism	0.01	0.01, 0.02	<.0001*	0.008	0.002, 0.01	.01*
Kmax	0.0009	-0.006, 0.008	.80	0.01	0.0006, 0.02	.03*
MCT	0.0003	0.0001, 0.0005	.002*	-0.001	-0.001, -0.0005	.0003*

Kmax = maximum keratometry; MCT = minimum corneal thickness

*Statistically significant

Variable	Group 1			Group 2			P value G1 vs G2 ^a
	Low vision preop (N = 14)	Low vision postop	P value	Low vision preop (N = 32)	Low vision postop	P value	
CDVA (logMAR)	0.51 ± 0.07	0.16 ± 0.02	<.001*	0.42 ± 0.06	0.15 ± 0.03	<.001*	.91
Sphere (D)	-5.80 ± 0.80	-3.40 ± 1.10	<.001*	-1.90 ± 0.10	-2.10 ± 0.60	.01*	.06
Astigmatism (D)	-6.70 ± 1.50	-5.50 ± 0.20	.008*	-5.10 ± 0.23	-4.90 ± 0.30	.02*	.37
Kmax (D)	55.00 ± 2.30	54.20 ± 0.40	<.001*	54.50 ± 0.30	53.60 ± 0.40	<.001*	.30
MCT (μm)	448.3 ± 24.5	401.9 ± 0.8	<.001*	454.1 ± 16.7	401.5 ± 0.5	<.001*	.72
Total HOAs RMS (μm)	3.2 ± 0.03	2.86 ± 0.02	<.001*	4.03 ± 0.24	2.9 ± 0.1	<.001*	.81
Coma RMS (μm)	1.9 ± 0.1	1.2 ± 0.02	<.001*	2.2 ± 0.7	1.1 ± 0.09	<.001*	.32
SA RMS (μm)	-1.7 ± 0.2	-0.15 ± 0.02	<.001*	-0.25 ± 0.37	-0.2 ± 0.3	.2*	.12

Coma RMS = coma root main square; HOA RMS = HOA root main square; Kmax = maximum keratometry; MCT = minimum corneal thickness; preop = preoperative; postop = postoperative; SA RMS = spherical aberration root main square All data were reported as mean ± SD

*Statistically significant

^aComparison between central and paracentral keratoconus with low vision after treatment

^bComparison between central and paracentral keratoconus with high vision after treatment

ablation was performed, considering its different thicknesses on the cone apex and periphery. This is mandatory to consider in the stromal regulation plan to not exceed the ablation limit depth and to preserve an RST more than 350 μm .

The goal of the corneal reshaping is to achieve the maximum correction of coma HOAs, eventually reducing spherical and cylinder correction, to not exceed the established ablation depth limit.²¹ In fact, to improve the reduction of coma aberrations, the ablation was set 1 mm from the corneal vertex in the direction of the cone apex, to center the ablation more on the cone apex about corneal vertex and to reduce stromal ablation over the cone apex.

Several authors demonstrated that cone location is one of the most important parameters involved in corneal flattening after CXL, reporting that more topographic flattening occurs in eyes with centrally located cones.^{15,16} We compared the results of the STARE-X protocol in centrally and paracentrally located keratoconus, demonstrating visual and refractive improvement maintained at 2 years after treatment in both groups, and a statistically significant change in HOAs was assessed (Table 2).

In addition to the biomechanical properties differences, the radiation beam pattern of the previous generation of the CXL devices plays a critical role, causing different energy absorption between central and paracentral cornea, more crosslinking effect, and, by time, flattening effect on the central cornea rather than cone apex.^{16,21-23}

The uneven energy delivery can be easily understood looking at demarcation line, deeper in the center and gradually becomes superficial going toward the periphery.^{15,16,22} The top-hat or umbrella-like beam produced by a newer CXL device significantly improved the energy management, delivering a more even amount of radiation from center to periphery and improving the crosslinking effect in the apex zone.²⁴

In the STARE-X protocol, the beam is centered on the cone apex, eventually covering the limbus with a sponge if the beam diameter exceeds the corneal limbus. The results are that demarcation line depth after this protocol is more even from center to periphery.²⁵

A customized and cone-centered irradiation profile will lead to a better CXL effect, more flattening in the apex zone, and, consequently, a better chance to aim to a better refractive effect.²⁶ In this study, at 2 years after treatment, a significant reduction of Kmax was observed in both groups.

The mean preoperative HOAs RMS was higher in paracentral KC, whereas SA RMS was prevalent in the central location; however, a statistically significant decrease of HOAs RMS and coma RMS was noted in both groups at 24 months. In addition, no statistically significant differences were observed in subgroup analysis comparing patients with preoperative low vision and good vision in both central and paracentral keratoconus.

No persistent corneal opacities were observed throughout the 2 years of follow-up in our group. According to the study by Kymionis et al., simultaneous CXL-plus leads to the various grades of keratocytes depopulation into the anterior stroma, reducing the risk for haze after treatment.²⁷

Furthermore, Krueger et al., regarding the advantages in clinical applications of accelerated CXL, reported reduced postoperative glare disability, subepithelial nerve plexus nerves damage, and less postoperative haze compared with standard protocol.²⁸ Previous studies on customized TG-CXL treatment described a significant lower apoptosis rate of keratocytes outside the cone and a higher nerve density and reported better tolerability of the customized treatments.^{29,30}

In conclusion, the STARE-X protocol demonstrated effective results in halting keratoconus progression, improving corneal regularity with a safe and effective profile. Our protocol treatment improved both visual acuity and corneal aberration at 2 years of follow-up. Longer follow-up is needed to observe further long-term CXL flattening effect on the cone. Moreover, this study confirmed the safety of the STARE-X protocol and its efficacy based on the stabilization of keratoconus progression in central and paracentral keratoconus. To the authors' knowledge, this is the first report that compared the results of transepithelial ablation for corneal regularization of keratoconus and simultaneous accelerated CXL, in central and paracentral location.

Table 5. Continued

Group 1			Group 2			P value G1 vs G2 ^b
High vision preop (N = 36)	High vision postop	P value	High vision preop (N = 18)	High vision postop	P value	
0.23 ± 0.06	0.07 ± 0.02	<.001*	0.25 ± 0.07	0.08 ± 0.02	<.001*	.51
-4.10 ± 0.70	-1.60 ± 0.80	<.001*	-0.70 ± 0.63	-0.44 ± 1.10	.17	.35
-4.50 ± 0.75	2.54 ± 1.32	<.001*	-4.20 ± 1.10	-4.10 ± 1.00	.001*	.04*
54.30 ± 0.40	53.10 ± 1.00	<.001*	53.40 ± 0.50	51.90 ± 0.60	<.001*	.02*
5050.3 ± 18.9	413.2 ± 15.7	<.001*	489.9 ± 17.8	410.3 ± 24.6	<.001*	.01*
2.95 ± 0.13	2.7 ± 0.1	<.001*	3.52 ± 0.3	2.7 ± 0.11	<.001*	.16
1.6 ± 0.1	0.75 ± 0.3	<.001*	1.6 ± 0.1	0.91 ± 0.22	<.001*	.25
-1.01 ± 0.33	-0.11 ± 0.04	<.001*	-0.07 ± 0.02	-0.05 ± 0.02	<.001*	.88

WHAT WAS KNOWN

- The combination of corneal crosslinking (CXL) and refractive treatment (CXL plus) demonstrated a significant reshaping of the irregular corneal surface and improvement of the visual function in keratoconus. However, no studies evaluated the differences between central and paracentral cone location.

WHAT THIS PAPER ADDS

- Selective transepithelial topography-guided photorefractive keratectomy combined with accelerated CXL described in this paper improved visual acuity, manifest refraction, and aberrometric outcomes in both central and paracentral keratoconus.
- However, at the end of follow-up, a better corrected distance visual acuity and a higher reduction of spherical aberration were observed in patients with central keratoconus.

REFERENCES

- Rabinowitz YS. Keratoconus. *Surv Ophthalmol* 1998;42:297–319
- Mazzotta C, Traversi C, Baiocchi S, Bagaglia S, Caporossi O, Villano A, Caporossi A. Corneal collagen crosslinking with riboflavin and ultraviolet A light for pediatric keratoconus: ten-year results. *Cornea* 2018;37:560–566
- Mazzotta C, Caporossi T, Denaro R, Bovone C, Sparano C, Paradiso A, Baiocchi S, Caporossi A. Morphological and functional correlations in riboflavin UV A corneal collagen cross-linking for keratoconus. *Acta Ophthalmol* 2012;90:259–265
- Moschos MM, Nitoda E, Georgoudis P, Balidis M, Karageorgiadis E, Kozeis N. Contact lenses for keratoconus-current practice. *Open Ophthalmol J* 2017;11:241–251
- Delgado S, Velazco J, Delgado Pelayo RM, Ruiz-Quintero N. Correlation of higher order aberrations in the anterior corneal surface and degree of keratoconus measured with a Scheimpflug camera. *Arch Soc Esp Oftalmol* 2016;91:316–319
- Dawson DG, Randleman JB, Grossniklaus HE, O'Brien TP, Dubovy SR, Schmack I, Stulting RD, Edelhauser HF. Corneal ectasia after excimer laser keratorefractive surgery: histopathology, ultrastructure, and pathophysiology. *Ophthalmology* 2008;115:2181–2191.e1
- Arba-Mosquera S, Merayo-Llodes J, de Ortueta D. Clinical effects of pure cyclotorsional errors during refractive surgery. *Invest Ophthalmol Vis Sci* 2008;49:4828–4836
- Bueeler M, Mrochen M. Simulation of eye-tracker latency, spot size, and ablation pulse depth on the correction of higher order wavefront aberrations with scanning spot laser systems. *J Refractive Surg* 2005;21:28–36
- Kanellopoulos AJ, Binder PS. Collagen cross-linking (CCL) with sequential topography-guided PRK: a temporizing alternative for keratoconus to penetrating keratoplasty. *Cornea* 2007;26:891–895
- Krueger RR, Kanellopoulos AJ. Stability of simultaneous topography-guided photorefractive keratectomy and riboflavin/UVA cross-linking for progressive keratoconus: case reports. *J Refract Surg* 2010;26:S827–S832
- Lin DT, Holland S, Tan JC, Moloney G. Clinical results of topography-based customized ablations in highly aberrated eyes and keratoconus/ectasia with cross-linking. *J Refract Surg* 2012;28:S841–S848
- Gore DM, Leucci MT, Anand V, Fernandez-Vega Cueto L, Arba Mosquera S, Allan BD. Combined wavefront-guided transepithelial photorefractive keratectomy and corneal crosslinking for visual rehabilitation in moderate keratoconus. *J Cataract Refract Surg* 2018;44:571–580
- Kymionis GD, Grentzelos MA, Portaliou DM, Kankariya VP, Randleman JB. Corneal collagen cross-linking (CXL) combined with refractive procedures for the treatment of corneal ectatic disorders: CXL plus. *J Refract Surg* 2014;30:566–576
- Kanellopoulos AJ. Comparison of sequential vs same-day simultaneous collagen cross-linking and topography-guided PRK for treatment of keratoconus. *J Refract Surg* 2009;25:S812–S818
- Greenstein SA, Fry KL, Hersh PS. Effect of topographic cone location on outcomes of corneal collagen cross-linking for keratoconus and corneal ectasia. *J Refract Surg* 2012;28:397–405
- Tian M, Ma P, Zhou W, Feng J, Mu G. Outcomes of corneal crosslinking for central and paracentral keratoconus. *Medicine (Baltimore)* 2017;96:e6247
- Zhu AY, Jun AS, Soiberman US. Combined protocols for corneal collagen cross-linking with photorefractive surgery for refractive management of keratoconus: update on techniques and review of literature. *Ophthalmol Ther* 2019;8(suppl 1):15–31
- Reinstein DZ, Archer TJ, Gobbe M, Silverman RH, Coleman DJ. Epithelial thickness in the normal cornea: three-dimensional display with Artemis very high-frequency digital ultrasound. *J Refract Surg* 2008;24:571–581
- Haque S, Simpson T, Jones L. Corneal and epithelial thickness in keratoconus: a comparison of ultrasonic pachymetry, Orbscan II, and optical coherence tomography. *J Refract Surg* 2006;22:486–493
- Reinstein DZ, Gobbe M, Archer TJ, Silverman RH, Coleman DJ. Epithelial, stromal, and total corneal thickness in keratoconus: three-dimensional display with Artemis very-high frequency digital ultrasound. *J Refract Surg* 2010;26:259–271
- Piccinini AL, Golan O, Torres-Netto EA, Hafezi F, Randleman JB. Corneal higher-order aberrations measurements: comparison between Scheimpflug and dual Scheimpflug-Placido technology in keratoconic eyes. *J Cataract Refract Surg* 2019;45:985–991
- Koller T, Schumacher S, Fankhauser F II, Seiler T. Riboflavin/ultraviolet a crosslinking of the paracentral cornea. *Cornea* 2013;32:165–168
- Yam JC, Cheng AC. Reduced cross-linking demarcation line depth at the peripheral cornea after corneal collagen cross-linking. *J Refract Surg* 2013;29:49–53
- Herber R, Kunert KS, Veliká V, Spoerl E, Pillunat LE, Raiskup F. Influence of the beam profile crosslinking setting on changes in corneal topography and tomography in progressive keratoconus: preliminary results. *J Cataract Refract Surg* 2018;44:718–724
- Mazzotta C, Traversi C, Paradiso AL, Latronico ME, Rechichi M. Pulsed light accelerated crosslinking versus continuous light accelerated crosslinking: one-year results. *J Ophthalmol* 2014;2014:604731
- Prakash G, Srivastava D, Choudhuri S, Thirumalai SM, Bacero R. Differences in central and non-central keratoconus, and their effect on the objective screening thresholds for keratoconus. *Acta Ophthalmol* 2016;94:e118–e129
- Kymionis GD, Portaliou DM, Kounis GA, Limnopolou AN, Kontadakis GA, Grentzelos MA. Simultaneous topography-guided photorefractive keratectomy followed by corneal collagen crosslinking for keratoconus. *Am J Ophthalmol* 2011;152:748–755
- Krueger RR, Herekar S, Spoerl E. First proposed efficacy study of high versus standard irradiance and fractionated riboflavin/ultraviolet A cross-linking with equivalent energy exposure. *Eye Contact Lens* 2014;40:353–357
- Cassagne M, Pierné K, Galiacy SD, Asfaux-Marfaing MP, Fournié P, Malecaze F. Customized topography-guided corneal collagen cross-linking for keratoconus. *J Refract Surg* 2017;33:290–297
- Mazzotta C, Baiocchi S, Bagaglia SA, Fruschelli M, Meduri A, Rechichi M. Accelerated 15 mW pulsed-light crosslinking to treat progressive keratoconus: two-year clinical results. *J Cataract Refract Surg* 2017;43:1081–1088

Disclosures: None reported.

First author:

Miguel Rechichi, MD, PhD

Centro Polispecialistico Mediterraneo, Sellia Marina, Italy

This is an open access article distributed under the Creative Commons Attribution License 4.0 (CCBY), which permits unrestricted use, distribution, and reproduction in any medium, provided the original work is properly cited.